Research article

Research on the zero-calibration gauge device

Zhichao Wu [a],[*], Furong Lei [a], Linan Wang [b], Yu Fu [b]

[a] *School of Optoelectronic Engineering, Xi'An Technological University, Xi'An, China*
[b] *Norinco Group Test and Measuring Academy, Shaanxi, Huayin, China*

A B S T R A C T

To meet the demand for the track's geometric parameter detection equipment for train speed and high-speed aerodynamics tests, a zero-calibration gauge device is designed with the centering limit, height adjustment and horizontal display function in this paper. The bending situation of the zero-calibration gauge is analyzed and the processing technology is studied, which ensures the rationality and realizability of the design of zero-calibration gauge. Then the gauge zero value and the parallelism of the working surface of zero-calibration gauge have been experimentally tested. The experimental results show that the parameter of gauge zero value is 1434.829 mm with a standard deviation of 1.4 µm. The parallelism of the two upper working surfaces is 1.1 µm, and the parallelism of the two inner working surfaces is 4 µm. Finally, the uncertainty evaluation of zero-calibration gauge is completed. The measurement uncertainty of gauge zero value is 12 µm and the measurement uncertainty of height difference is 6 µm.

1. Introduction

With the increase in train speed [1]and the demand for high-speed aerodynamic tests [2], there is a higher and higher demand for the track's geometric parameter detection technology [3], such as a track gauge with higher measurement accuracy [4] and a dynamic track measuring device for gauge [5]. For any track measurement equipment, the gauge zero value and ultrahigh value [6], as the most basic parameters, must be guaranteed very high accuracy. Otherwise, it will seriously affect the measurement accuracy. Due to the complex meteorological conditions of temperature, humidity, air temperature, light and other conditions in the field [7], the performance of the measuring instrument will change greatly and the zero value of the instrument will drift. Before using the detection instrument, the zero-value calibration verification of the instrument is necessary to ensure the accuracy of testing data. Therefore, designing a high-precision zero-calibration gauge device is of great significance and engineering value.

The existing way of gauge calibration is mainly using the railroad gauge calibration [8], which can calibrate the ultrahigh value and gauge zero value, etc. The traditional calibrator [9] is complicated to operate, and the material used is ordinary steel, which has a significant coefficient of thermal expansion, and the calibration accuracy is greatly affected by temperature. The error of the gradeIcalibration [10]on the ultrahigh value calibration of the gauge is about 0.04 mm, and the maximum error on the gauge calibration is about 0.05 mm. The device designed by H. Chen et al. [11] has the advantages of automatic detection, high degree of intelligence, and a wide range of measurement parameters, but the accuracy of measuring gauge is 0.06 mm, and the accuracy of ultra-high is 0.30 mm. Li Chao et al. [12]used the block gauge calibrator to measure the gauge with an accuracy of 0.036 mm and an ultra-high accuracy of 0.072 mm, but this device is complicated. The automatic calibration and alignment system developed by Wang Min et al. [13]designed
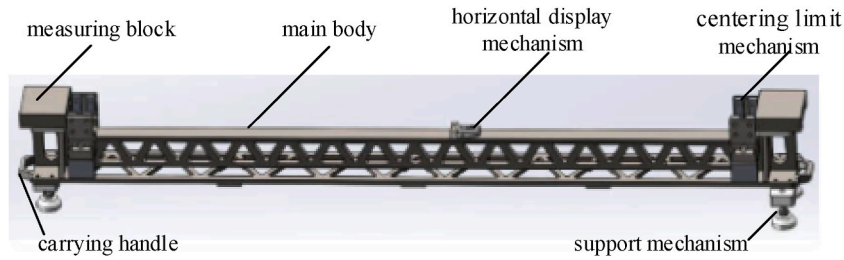

Fig. 1. The construction of zero-calibration gauge device.

an automatic calibration and alignment system for the gauge, which had high adjustment flexibility and can detect multiple data at the same time. However, the system still does not have a horizontal display and centering limit. In brief, the zero-value calibration device has some problems, such as a large coefficient of thermal expansion, side bending of the single vertical beam, no horizontal display, no centering limit, etc.

Responding to the existing problems and shortcomings, a zero-calibration gauge device with higher accuracy and more comprehensive functions is designed in this paper, which can make up for the defects of available zero value calibration devices.

2. Design of device

The zero-calibration gauge device consists of the main body, measuring block, centering limit mechanism, support mechanism, horizontal display mechanism and carrying handle. The reference value of the gauge zero parameters is 1435 mm, the dimension is 1653mm × 213mm × 271 mm, and the total weight is about 35.6 kg.

The design of zero-calibration gauge is shown in Fig. 1.

The main body is made of 4J32A material, also known as Super-Invar alloy. The material has a small coefficient of thermal expansion and can work in a large temperature difference environment. The working surfaces inside the measuring block at both ends are parallel, the theoretical distance is 1435 mm, and the upper working surfaces of the two measuring blocks are coplanar. Using the special shape relationship between the working surfaces of the two measuring blocks, the gauge zero value and ultrahigh value of the gauge can be calibrated. The support mechanism and the horizontal display mechanism can achieve the level adjustment and the display function. The centering limit mechanism can realize the centering and limiting function of the calibrated equipment. When calibrating the zero value of gauge, it can make the gauge in the correct position. The axis of the gauge is coincident with the calibration axis of zero-calibration gauge to improve the accuracy.

3. Processing technology

The most important structures in the zero-calibration gauge are the main body and the measuring block, which directly affect the performance and accuracy of the zero-calibration gauge. Therefore, reasonable processing technology and process must be considered when designing the zero-calibration gauge.

1)Using the waterjet cutting to machine each part blank of the main body according to the size of the drawing dimensions, with a 5 mm machining allowance. 2)Using the CNC(Computerized Numerical Control) to mill the shape and triangle holes. 3)Argon arc welding and heat treatment of the main body. 4)Sand blasting. 5)Finishing the main body and processing the back tab by the milling planer to ensure coplanarity. Grinding the mounting surfaces of both ends to make them equal and parallel. 6)Machining both ends of the measuring blocks, leaving a margin after rough machining, conducting vacuum quenching, tempering to the drawing hardness, and flat grinding process each plane. 7)Installing the measuring block. After leveling, testing the parallelism, perpendicularity and flatness of the two mounting blocks, and if necessary, grinding until qualified. 8) Using argon arc welding to weld the main body and the measuring block. 9) Measure again and grind if necessary. 10) Waiting for the final measurement after 2 days later and installing the accessories after qualified. The device is completed.

4. Force analysis

The zero-calibration gauge is simplified to a simply supported beam model subjected to a uniform load. In transverse force bending, bending moments and shear forces are in the beam cross-section. But for slender beams, the strain energy in shear is generally small compared to the bending strain energy, so that it can be negligible [14]. The shape of the device and its loading force are symmetrical, so torsion is also insignificant.

The approximate differential equation of the deflection curve can be applied to find its equation, as shown in Eq. (1).

$$EIw = \frac{ql}{12}x^3 - \frac{q}{24}x^4 + Cx + D \tag{1}$$

where E is the modulus of elasticity of the material, I is the moment of inertia of the material, w is the deflection in the beam span, q is

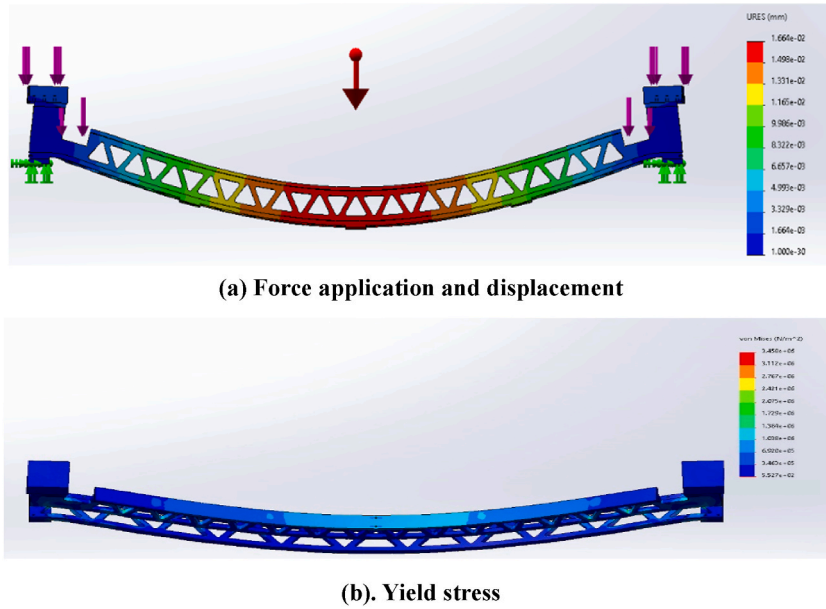**(a) Force application and displacement**

(b). Yield stress

Fig. 2. Force analysis of the zero-calibration gauge device
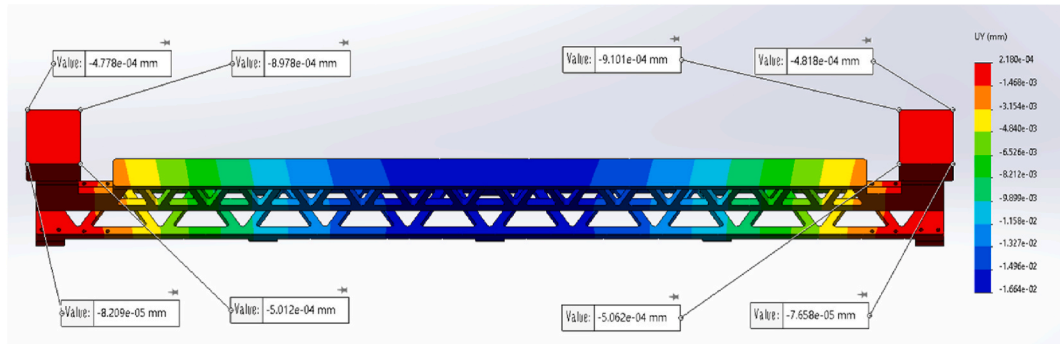(a) Force application and displacement
(b). Yield stress.

Fig. 3. Changes in relative displacement of the upper working surface of the zero-calibration gauge device.

the standard value of uniform wiring load, l is the span of the simply supported beam, x is the displacement at any point of the beam section, C and D are integration constants.

Boundary conditions: the deflection on the support is equal to zero and the slope of the tangent to the deflection curve at the midpoint of the span is equal to zero.

Substituting the deflection curve equation, an extreme value is obtained for the deflection at the midpoint of the span, as shown in Eq. (2).

$$w_{max} = -\frac{5ql^4}{384EI} \tag{2}$$

where w_{max} is the maximum deflection in the beam span, l is the span of the simply supported beam, q is the standard value of uniform wiring load, E is the modulus of elasticity of the material, I is the moment of inertia of the material.

Therefore, the maximum deformation w_{max} can be calculated as -12.23 μm.

The bending moment in transverse force bending changes depending on the position of the section. And the section with the largest bending moment is generally the area with the highest positive stress. Thus, the strength demands for bending positive stresses during strength calibration are Eq. (3).

$$\sigma_{max} = \frac{M_{max}}{W} \leq [\sigma] \tag{3}$$

3

Table 1

The measured data of the two upper working surfaces.

Number	Measuring block1			Measuring block2		
	x_i (mm)	y_i (mm)	z_i(μm)	x_i(mm)	y_i (mm)	z_i (μm)
1	5	5	50	1440	5	49
2	30	5	50	1465	5	49
3	60	5	49	1495	5	49
4	90	5	49	1525	5	49
5	5	30	50	1440	30	50
6	30	30	50	1465	30	50
7	60	30	50	1495	30	49
8	90	30	50	1525	30	49
9	5	60	50	1440	60	50
10	30	60	50	1465	60	49
11	60	60	50	1495	60	48
12	90	60	49	1525	60	49
13	5	90	50	1440	90	50
14	30	90	50	1465	90	49
15	60	90	49	1495	90	49
16	90	90	49	1525	90	48
17	5	120	50	1440	120	49
18	30	120	50	1465	120	50
19	60	120	49	1495	120	49
20	90	120	50	1525	120	48

where M_{max} is the maximum bending moment, W is he coefficient of flexural section of the material, $[\sigma]$ is the permissible stress of the material.

The maximum bending moment of the simply supported beam with uniform load is $Ql^2/8$, calculated as 92.981 N·m, and the estimated bending section factor is $3.292 \times 10^{-5} m^3$, then σ_{max} is 2.824 MPa, which is much less than the material's yield stress of 302 MPa.

SolidWorks software is used to analyze the zero-calibration gauge, and pressure is used instead of the centering limit mechanism. A force of 300 N is applied to the working surface on the measuring block, and the direction of the applied force is vertically downward, as shown in Fig. 2(a). The yield stress diagram is shown in Fig. 2(b).

As can be seen from Fig. 2, the maximum deformation of the zero-calibration gauge is 16.64 μm, and the zero value of the gauge brought by this deformation is about 4×10^{-7}mm, which can be ignored. A simplified model is used for the theoretical calculations in the static stress analyses, and the weight reduction structure is also neglected. So, the maximum deformation and stress values obtained from the simulation are slightly larger.

The relative displacement of each vertex on the upper working surface of the zero-calibration gauge in the Y-axis direction is shown in Fig. 3. The parallelism error of the two upper working surfaces of the zero-calibration gauge due to deformation is 0.83 μm.

Similarly, the parallelism error of the two inner working surfaces of the gauge due to deformation is 0.65 μm. In summary, the force deformation of the device is very small and can be ignored, which proves that the material selection and design of the device are reasonable.

5. Experiments and analysis of results

The zero-calibration gauge is placed on the 00-grade marble platform and kept level. The length direction, the width direction and the height direction of the zero-calibration gauge are defined as the x-axis, the y-axis and the z-axis. After using the dial test indicator to measure the height values of multiple points on the two working surfaces of the zero-calibration gauge, the data obtained is processed to calculate the parallelism error of the two upper working surfaces. The measurement points of the measured plane are $(x_i, y_i, z_i)(i = 1, 2, \cdots, k)$. The reference plane is established assuming that the equation of the reference plane is Eq. (4).

$$z_i = ax_i + by_j + c \tag{4}$$

where a, b, c are the parameters of the plane equation.

According to the principle of the least squares method [15], it is necessary to minimize the sum of squared deviations of all measured values on the measured surface from the plane, as shown in Eq. (5).

$$F(a,b,c) = \sum_{i=1}^{k} (z_i - ax_i - by_i - c)^2 = min \tag{5}$$

where $F(a,b,c)$ is the minimization value.

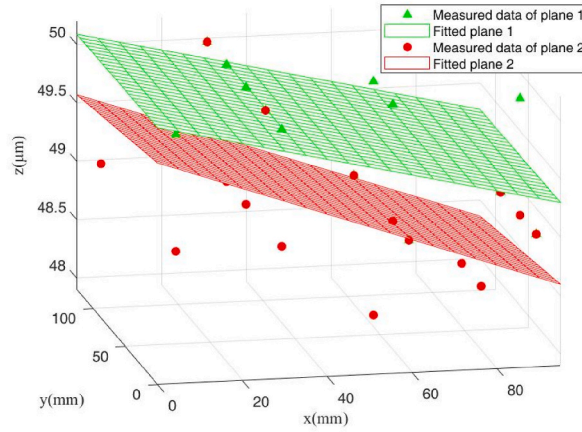And the parameters a, b, c of the ideal plane equation are obtained by Eq. (6).

Fig. 4. The simulated graph of the two upper surfaces.

Table 2
The measurement data of the zero value of gauge.

Number	y (mm)	z (mm)	x_1 (mm)	x_2 (mm)	l (mm)	L (mm)
1	5	4	0.004	0.005	1432.76	1434.829
2	5	12	0.008	0.009	1432.769	1434.83
3	5	20	0.006	0.008	1432.763	1434.827
4	5	28	0.007	0.002	1432.762	1434.831
5	30	4	0.004	0.004	1432.757	1434.827
6	30	12	0.002	0.008	1432.761	1434.829
7	30	20	0.008	0.008	1432.765	1434.827
8	30	28	0.008	0.002	1432.76	1434.828
9	60	4	0.006	0.006	1432.762	1434.828
10	60	12	0.004	0.008	1432.764	1434.83
11	60	20	0.005	0.004	1432.759	1434.828
12	60	28	0.008	0.007	1432.766	1434.829
13	90	4	0.01	0.008	1432.77	1434.83
14	90	12	0.009	0.008	1432.77	1434.831
15	90	20	0.007	0.007	1432.765	1434.829
16	90	28	0.008	0.003	1432.764	1434.831
17	120	4	0.006	0.008	1432.763	1434.827
18	120	12	0.008	0.008	1432.768	1434.83
19	120	20	0.006	0.004	1432.76	1434.828
20	120	28	0.005	0.009	1432.765	1434.829

The arithmetic mean of the above measurement data is about 1434.829 mm, as the distance between the two inner working surfaces of the zero-calibration gauge, and the standard deviation is calculated to be 1.4 μm.

$$
\begin{bmatrix}
\sum_{i=1}^{k} x_i^2 & \sum_{i=1}^{k} x_i y_i & \sum_{i=1}^{k} x_i \\
\sum_{i=1}^{k} x_i y_i & \sum_{i=1}^{k} y_i^2 & \sum_{i=1}^{k} y_i \\
\sum_{i=1}^{k} x_i & \sum_{i=1}^{k} y_i & k
\end{bmatrix}
\begin{bmatrix} a \\ b \\ c \end{bmatrix}
=
\begin{bmatrix}
\sum_{i=1}^{k} x_i z_i \\
\sum_{i=1}^{k} y_i z_i \\
\sum_{i=1}^{k} z_i
\end{bmatrix}
\tag{6}
$$

where a, b, c are the plane equation parameters and (x_i, y_i, z_i) is the measured data of the measured plane.

Then the parallelism error is $max\{z_{ij}\} - min\{z_{ij}\}$. In this paper, based on the least squares method, the ideal plane is found using the Matlab software, which can be used as a benchmark for the parallelism error evaluation.

The measured data of the two upper working surfaces are shown in Table 1.

Fitting the plane according to the data in Table 1, the equations are Eq. (7) and Eq. (8), respectively.

$$
\text{Plane 1}: z = -0.0085x - 1.1876 \times 10^{-4}y + 50.0994
\tag{7}
$$

$$
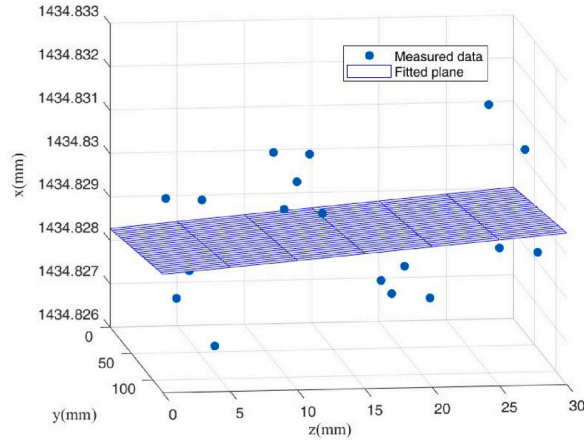\text{Plane 2}: z = -0.0127x - 0.0018y + 49.7977
\tag{8}
$$

Fig. 5. The simulated graph of the plane.

The parallelism between the two upper working surfaces of the zero-calibration gauge is calculated to be 1.1 μm. In order to display the height difference between two working surfaces more intuitively, the X coordinates are processed in drawing, as shown in Fig. 4.

The zero value of the zero-calibration gauge is measured by using the laser interferometer and the dial test indicator. The zero value of the gauge can be obtained by Eq. (9).

$$L = l + d - (x_1 + x_2) \tag{9}$$

where L is the zero value of the gauge, l is the measured data by the laser interferometer, d is the probe diameter of the dial test indicator 2.078 mm, x_1, x_2 are the display data of the dial test indicator contacting the two ends of the zero-calibration gauge, respectively.

The measurement data of the zero value of the gauge are shown in Table 2.

The plane equation fitted to the data above is Eq. (10).

$$x = 3.7708 \times 10^{-6} y + 2.5 \times 10^{-5} z + 1.434 \times 10^3 \tag{10}$$

The simulated graph is shown in Fig. 5.

As can be seen from Fig. 5, the farthest point above the plane is 2.1 μm from the plane, and the farthest point below the plane is 1.9 μm from the plane. Therefore, the parallelism of the inside working surface of the zero-calibration gauge is 4 μm.

6. Measurement uncertainty evaluation

As a measuring instrument, it is necessary to evaluate the uncertainty of the zero-calibration gauge. Due to the zero-calibration gauge is mainly to calibrate the zero value and the ultrahigh value of the gauge, therefore, the uncertainty of the gauge zero parameters and the height difference of the two measuring blocks on the working surface should be analyzed separately [16].

1) Evaluation of measurement uncertainty of the gauge zero parameter

The main sources of measurement uncertainty are as follows. a. The uncertainty component u_1 introduced by the error of display value of dial test indicator. The resolution of the lever micrometer is 0.001 mm, obeying the uniform distribution, and the coverage factor k is $\sqrt{3}$, then u_1 is 0.0003 mm b. The uncertainty component u_2 introduced by the material coefficient of thermal expansion. The coefficient of thermal expansion α of the calibration device is $1.1 \times 10^{-6}/°C$, the corrected temperature variation range Δt is $\pm 1 °C$, obeying the uniform distribution, then u_2 is $1653mm \times \alpha \times \Delta t / \sqrt{3}$, calculated as 0.001 mm. c. The uncertainty component u_3 introduced by the measurement axis deviation. The measurement axis deviation is 0.0005 mm, obeying a uniform distribution, then u_3 is 0.0003 mm. d. The uncertainty component u_4 introduced by the display value of laser interferometer [17]. The error of the value of the laser interferometer is 0.0005 mm, obeying a uniform distribution, then u_4 is 0.0002mm. e. The uncertainty component u_5 introduced by the Abbe error. The straightness error of the screw is $10''$, and the Abbey off-axis amount is 80 mm, so the Abbey error is 0.0038 mm, obeying a uniform distribution, then u_5 is 0.0022 mm. f. The uncertainty component u_6 introduced by the straightness of slide rail. The width of the permissible size error is 0.010 mm, obeying a uniform distribution, then u_6 is 0.057 mm. g. The uncertainty component u_7 introduced by the repeatability measurement. According to Bessel's formula, the standard deviation is calculated to be 0.0011 mm, based on the class A evaluation method, then u_7 is 0.0012 mm. Assuming that the components are uncorrelated, the combined standard uncertainty is 0.0062 mm. And the extended uncertainty is $0.0124mm(k = 2)$.The uncertainty sources and estimations of the gauge zero value measurement are shown in Table 3.

Since each uncertainty source is unrelated to each other, then the combined standard uncertainty is 6.2 μm. The extended

Table 3

Uncertainty sources and estimations of the gauge zero value measurement.

Uncertainty sources	Uncertainty estimations (μm)
Display value of the dial test indicator	0.3
Material coefficient of thermal expansion	1.0
Measurement axis deviation	0.3
Display value of the laser interferometer	0.2
Abbe error	2.2
Straightness of the slide rail	5.7
Measurement repeatability	1.2
Combined standard uncertainty	6.2
Extended uncertainty	12.4

Table 4

Uncertainty sources and estimations of the height difference measurement.

Uncertainty sources	Uncertainty estimations (μm)
Display value of the dial test indicator	0.6
Measurement platform	2.9
Measurement repeatability	1.1
Combined standard uncertainty	3.2
Extended uncertainty	6.4

uncertainty is about 12 μm (k = 2).

2) Evaluation of measurement uncertainty of the height difference

The main sources of measurement uncertainty are as follows. a. The uncertainty component u_1 introduced by the error of the display value of dial test indicator. The error of the display value of dial test indicator is 0.002 mm, obeying the uniform distribution, and the coverage factor k is $\sqrt{3}$, then u_1 is 0.0006 mm. b. The uncertainty component u_2 introduced by the error of measurement platform. The error introduced by the measurement platform is 0.005 mm, obeying the uniform distribution, then u_2 is 0.0029 mm. c. The uncertainty component u_3 introduced by the repeatability measurement. According to Bessel's formula, the standard deviation is calculated to be 0.0011 mm, based on the class A evaluation method, then u_3 is 0.0011 mm. Assuming that the components are uncorrelated, the combined standard uncertainty is 0.0032 mm. And the extended uncertainty is $0.0064 mm (k = 2)$. The uncertainty sources and estimations of the height difference measurement are shown in Table 4.

Since each uncertainty source is unrelated to each other, then the combined standard uncertainty is 3.2 μm. The extended uncertainty is about 6 μm ($k = 2$).

7. Conclusion

In this paper, a zero-calibration gauge device that has the centering limit, the height adjustment and the horizontal display function was designed. In order to ensure the rationality and realizability of the designed device, its force bending situation was analyzed and the machining process was studied. The gauge zero value and the parallelism of the working surface of the zero-calibration gauge were experimentally measured. The test results showed that: (1) the parameter of gauge zero value is 1434.829 mm with a standard deviation of 1.4 μm; (2) the parallelism of the two upper working surfaces is 1.1 μm; (3) the parallelism of the two inner working surfaces is 4 μm; (4) Uncertainty evaluation shows that the measurement uncertainty of gauge zero value is 12 μm and the measurement uncertainty of height difference is 6 μm.

Data availability

All data generated or analyzed during this study are included in this article.

CRediT authorship contribution statement

Zhichao Wu: Writing – original draft. **Furong Lei:** Writing – original draft. **Linan Wang:** Writing – original draft. **Yu Fu:** Writing – original draft.

Declaration of competing interest

The authors declare the following financial interests/personal relationships which may be considered as potential competing interests:Z. C. Wu reports was provided by the Basic scientific research projects of National Defense Science, technology and industry. If

there are other authors, they declare that they have no known competing financial interests or personal relationships that could have appeared to influence the work reported in this paper.

Acknowledgements

References

[1] X. M Zhou, X.D. Lin, X.F. Ji, Effects of high-speed railway construction and operation on related industries in China, Sustainability 13 (11) (2021) 6119.
[2] S. Walia, V. Satya, S. Malik, S. Chander, S. Devi, A.C. Sharma, Rocket sled based high speed rail track test facilities, Defence Sci. J. 72 (2) (2022) 182–194.
[3] J.C. Nielsen, E.G. Berggren, A. Hammar, F. Jansson, R. Bolmsvilk, Degradation of railway tra-ck geometry-correlation between track stiffness gradient and differential settlement, Pro. IMechE Part F: J Rail and Rapid Transit 234 (1) (2020) 108–119.
[4] Janka Šestáková, Martin Mečár, Evaluation of Track Design and Track Geometry of the Track with Unconventional Structure of Railway Superstructure, Elsevier BV, 2015, pp. 709–716.
[5] Y. Tsubokawa, T. Ishikawa, Development of a dynamic track measuring device for gauge and twist to reduce derailment accidents, WIT Trans. Built Environ. 181 (2018) 253–262.
[6] L. Peng, S. Zheng, P. Li, Y. Wang, Q. Zhong, A comprehensive detection system for track geometry using fused vision and inertia, IEEE T INSTRUM MEAS 70 (5004615) (2021) 1–15.
[7] J. Calle-Sanchez, M. Molina-Garcia, J.I. Alonso, A. Fernamdez-Duran, Long term evolution in high speed railway environments: feasibility and challenges, Bell Labs Tech. J. 18 (2) (2013) 237–253.
[8] Chinese standard JJG 404-2008, Calibrators for Railway Track, China National Standard, Beijing, China, 2008.
[9] Y.C. Wang, M. Lu, Interpretation of JJG 404-2015 railway gauge calibrator, Railw. Tech. Supervision 44 (9) (2016) 18–20.
[10] H. Chen, W. Zou, Feasibility verification of portable intelligent gauge calibrator, JPCS 1802 (2) (2021) 22–41;
    [10a] H. Shi, M. Xu, Z. Yu, Track gauge measurement method based on least-square curve fitting theory, Tiedao Xuebao J. China Railw. Soc. 41 (2019) 81–88.
[11] H. Chen, W. Zou, Feasibility verification of portable intelligent gauge calibrator, JPCS 1802 (2) (2021) 22–41.
[12] Li chao, Wang chen, Zhou yi, Application of block gauge type railway gauge calibratior, Tiedao Xuebao J. China Railw. Soc. 49 (9) (2021) 10–14.
[13] Wang Min, Tang Xiaocong, CN Patent, 2022 114808574B. November 25.
[14] Hongwen Liu, Mechanics of MaterialsI, fifth ed., Higher Education Press, Beijing, 2011, pp. 142–187.
[15] C.M. He, X.R. Li, Y.Y. Hu, Z.C. Ye, H.G. Kang, Microscope images automatic focus algorithm based on eight-neighborhood operator and least square planar fitting, Optik 206 (2020) 164232.
[16] J. Cao, H. Li, X. Zhang, Calculation model and uncertainty analysis of projectile explosion position based on acousto-optic compound detection, Optik 253 (2022) 168822.
[17] R. Schnabel, Squeezed states of light and their applications in laser interferometers, Phys. Rep. 684 (2017) 1–51.